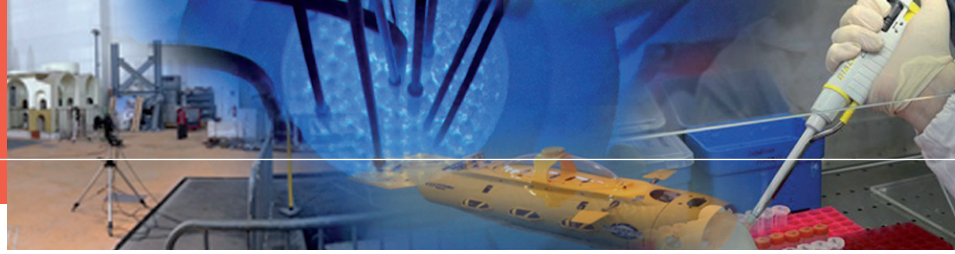

RF detection and anomalous heat production during electrochemical loading of deuterium in palladium

The production of excess power during electrochemical loading of palladium with deuterium was discovered in 1989 by Prof Martin Fleischmann and Prof Stanley Pons. In this article a picture of the research activities performed to correlate the effect and the material status is given. The structures of the electrochemical interface during the excess event and in the absence of excess power are compared, revealing a resonant equivalent circuit when the electrode is active. RF signals have also been detected when the anomalous heat production takes place

DOI 10.12910/EAI2014-62

Vittorio Violante, Emanuele Castagna, Stefano Lecci, Guglielmo Pagano, Mirko Sansovini, Francesca Sarto

Introduction

The phenomenon of excess power production during electrochemical loading of deuterium in palladium (in the past labeled as cold fusion, even if so far a clear signature in this direction is not yet available), is not yet understood, although during the last two decades in several calorimetric experiments the effect was observed to be well above the measurement uncertainties. The lack of reproducibility has been so far responsible for the absence of a clear explanation of the phenomenon.
The study performed during the last decade highlighted that the reproducibility of the effect is related with the status of the material. Upon examination of the cathodes that produce excess power, and of those made by a variety of techniques that do not produce excess power, many differences were noted that we believe are responsible for the lack of excess power results. Specifically: texture of the foils, grain size, crystal orientation, presence of impurity elements in Pd, surface morphology and roughness.
These differences were noted by performing many analyses including Scanning Electron Microscopy (SEM), X Ray Photoelectron Spectroscopy (XPS), confocal microscopy, Inductively Coupled Plasma (ICP)-Mass Spectroscopy (ICP-MS), Electron Backscattering Spectroscopy (EBSD), X Ray Fluorescence Spectroscopy (XRF), Raman Spectroscopy, Atomic Force Microscopy (AFM), and Angle Resolved Optical Scattering. Thus, prior research has shown that the occurrence of the effect is correlated with the material properties of the cathodes. Excess heat production was observed in different laboratories when using the same palladium-based material to manufacture the cathodes of the electrolytic cell. Analogously, negative results have been observed when using cathodes having different characteristics. In particular, it was found that a very high deuterium concentration in palladium (not less than 0.9 atomic fraction) was a necessary condition to observe the effect [1].

Vittorio Violante, Emanuele Castagna, Stefano Lecci, Guglielmo Pagano, Mirko Sansovini, Francesca Sarto
ENEA, Technical Unit for Nuclear Fusion

A metallurgical process developed at ENEA in order to optimize the hydrogen isotopes solubility in palladium [2-7] proved to be instrumental to the purpose. Furthermore, surface morphology (identified by means of power spectral density function -PSDF-), crystal orientation and mass transfer properties were identified to be correlated with the occurrence of the effect. The experimental results highlighted that the cathode behavior is significantly affected by the initial status of the material. For this reason a continuation of the study would be very helpful in order to get deeper into understanding the mechanisms responsible for the occurrence of the effect and to identify the features of the rough material that may affect the mechanisms, whether positively or negatively.

The spectrum of contaminants has been correlated to the material features since contaminants may act on crystal orientation, grain size, mass transfer and surface morphology as they modify the effect of chemical etching. Such a scenario has led to the production of doped palladium and palladium alloys.

A recent study [8] performed in ENEA did reveal that also the interface electrochemical equivalent circuit modifies at the onset of the effect: a resonant circuit structure has been identified inside the equivalent circuit.

Excess power:

1) Is a threshold effect (loading D/Pd > 0.9)
2) Is not observed with hydrogen
3) Is unexplainable as chemical effect
4) Occurs only if materials are showing specific characteristics as proper crystal orientation, proper structure of the grain boundaries, defined surface morphology, enhanced hydrogen isotopes mass transfer
5) Gives evidence that the cathode is undergoing resonance of some kind during excess heat events as measured by RF emission and by electrochemical impedance spectroscopy [8, 13].

A primary characteristic is the fact that there are high frequency resonance phenomena driven by electrolysis that play a role in any mechanism of FPE and have gone essentially undiscovered until now.

Another characteristic is the fundamental role played by material science. Indeed we believe that material status is the key to observe the effect and material science plays a key role to understand it, since some material characteristics support some processes rather than others.

Experimental evidence and electrochemical oscillations during an excess power event

Material science research led to the conclusion that some contaminants are necessary to increase the probability to observe the onset of the effect [8]. As rhodium addition produced remarkable results [9], then Pd90Rh10 cathodes have been prepared by applying the protocol developed at the Naval Research Laboratory (NRL) [13]. Palladium and Rhodium have been melted at 90/10 atomic ratio in an alumina crucible by using a Oxyacetylene torch. Material annealed 900 °C 2h, then rolled to 1 mm, then annealed again 900 °C 2h, then rolled to 50 microns and annealed as always. After rolling, the sample was annealed again at 850 °C and then etched with Aqua Regia. Figure 1 shows the surface of sample L119(20-60) after chemical etching.

Figure 2 shows the PSD of the surface of L119(20-60). PSD have been calculated by using AFM images.

A calorimetric study on sample L119(20-60) was performed by using the differential calorimeter developed at NRL [10], and the time trend of both input and output power is shown in Figure 3: here, excess power spontaneously develops after ~2.90E+5 s elapsed time and remains stable for about 12 hr. The possible effect due to a bias shift of the calorimetric system was checked by inverting the current and de-loading the cathode. When the cathode was de-loaded an input power level was applied as close as to the one existing before changing the polarity. After the thermal transient (with some adjusting of the input power at the required level), a perfect balance between power input and output was observed, i.e. the input and output curves were overlapping as shown in Figure 3. This confirmed that the signal was a real effect.

The polarity was then reversed again and PdRh was reloaded at a higher current value. As soon as the cathode was reloaded (~355000 s elapsed time) the system again produced an excess power event that was larger than the previous one.

Figure 4 shows the same calorimetric run after 5.30E+5

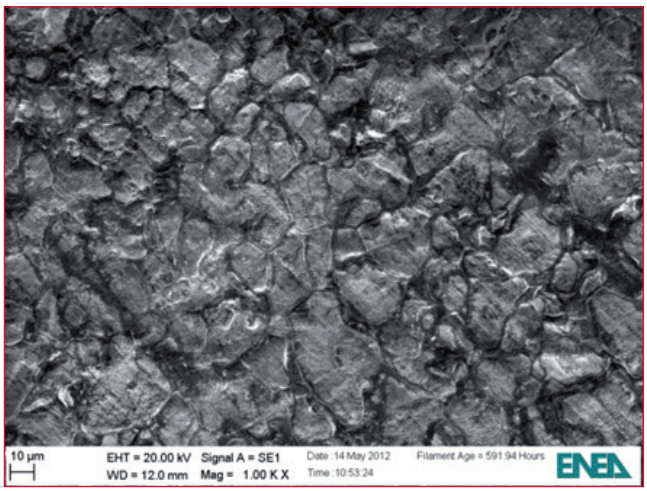

FIGURE 1 Surface of L119(20-60) $Pd_{90}Rh_{10}$

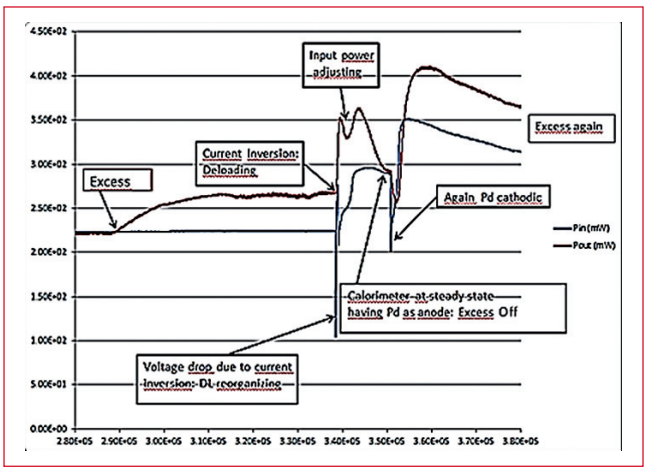

FIGURE 3 Excess power occurs (~2.90E+5-3.55E+5 s) and is switched off by current inversion. Restoring the original cathodic polarization restarts the excess power

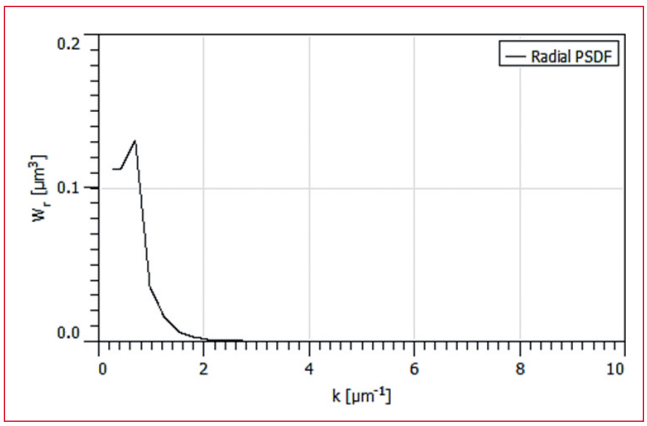

FIGURE 2 Power spectral density of L119(20-60)

s. After ~5.80E+5 s it was decided to perform a Galvanostatic Electrochemical Impedance Spectroscopy (GEIS) measurement by using the Biologic VP 200 Galvanostat-Potentiostat electrochemical spectrometer that was powering and controlling the experiment. This operation was performed in order to extract in situ new information on the status of the electrochemical interface in terms of an equivalent circuit.

The GEIS measurement was carried out within the frequency range 200 kHz-20 Hz and the Nyquist plot is shown in Figure 5a, with frequency decreasing from left to right in the plot. Figure 5a shows the equivalent circuit during the excess event and clearly a resonating component is contained. The applied DC current during the measurement was 90 mA, with a 7 mA sine probe amplitude.

Then the current was reduced to 30 mA DC and a time longer than the thermal transient of the calorimetric equipment was allowed to elapse. As can be seen from Figure 4, the excess power disappeared, then a new impedance analysis was performed and 25 Nyquist plots were acquired within the frequency range 400 kHz-10 Hz. Most of the plots were unstable yielding very scattered points as during the excess event. In some cases, as for instance in Figure 5a, it was possible to extract a clear signal.

Figures 5b and 5c show that the interphase structure was maintained also when the current was reduced to 30 mA (3 mA sine wave probe) although the excess power switched off. The resonating RLC structure disappeared from the impedance spectrum (always performed at 30 mA and by applying 3 mA sine wave probe) as soon as the input power was set to null for a few seconds before performing the GEIS again (see Figure 6).

The surprising result, even if preliminary, is that the excess power is characterized by a specific electrochemical structure of the interface (equivalent circuit) that may survive also after switching off the effect by redu-

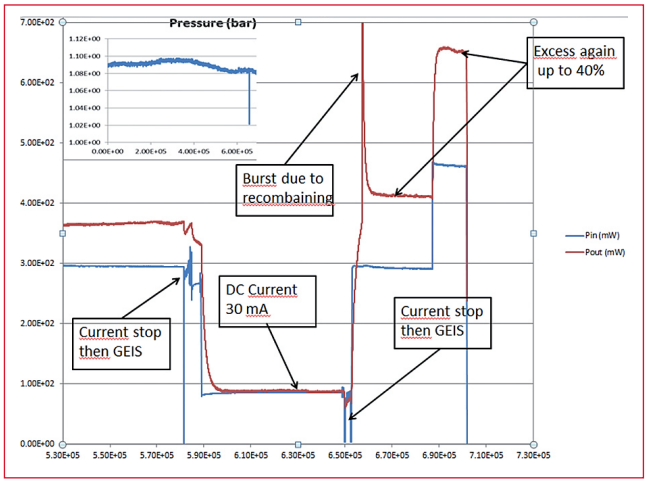

FIGURE 4 Excess power for the same run as in Fig. 3 at longer time

cing the current, but such a structure is destroyed if the system is more strongly perturbed by reducing the current to zero.

The inductive behavior in Figure 6 (negative imaginary component) at high frequencies is due to the wiring and connection of the cell and perfectly reproduces the tests performed with dummy circuits.

These preliminary results demonstrate that the electrochemical interface substantially changes during the production of excess power, and that the presence of LRC components suggests a resonant mechanism at the interface.

Figure 7, as a reference, shows a GEIS at two different current levels, performed on an inactive Pd cathode.

Further increasing the current produced greater excess power up to approximately 40% of the input.

The cell was switched off during the excess in order to physically investigate the status of the sample surface during an excess power event. Figure 8a shows a SEM image of the electrode L119(20-60) surface as it was during the excess. The electrode was removed from the cell during the excess without switching off the cathodic polarization. We observed a significant changing of the surface morphology given by dendrites deposition.

Figure 8b shows the PSD. The most significant peaks are in the region of wave number (k) up to about 5 μm^{-1} [3-5]; however surface study performed by nanoscope on

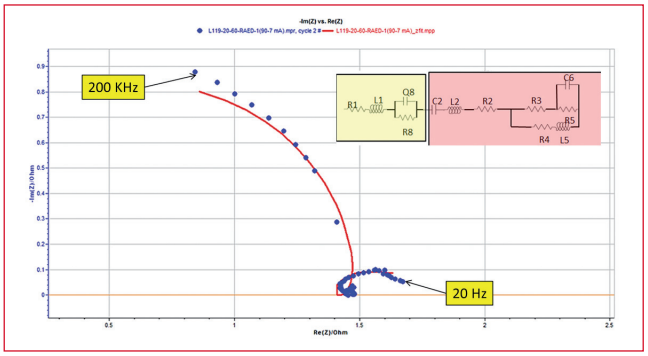

FIGURE 5A In situ Galvanostatic Electrochemical Impedance Spectroscopy on Sample L119(20-60). Excess-on. ω_R = 200 kHz

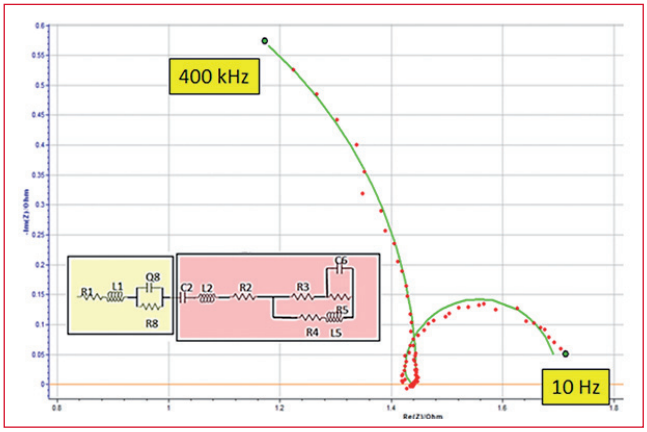

FIGURE 5B In situ Electrochemical Impedance Spectroscopy on Sample L119(20-60). Excess-off before perturbing

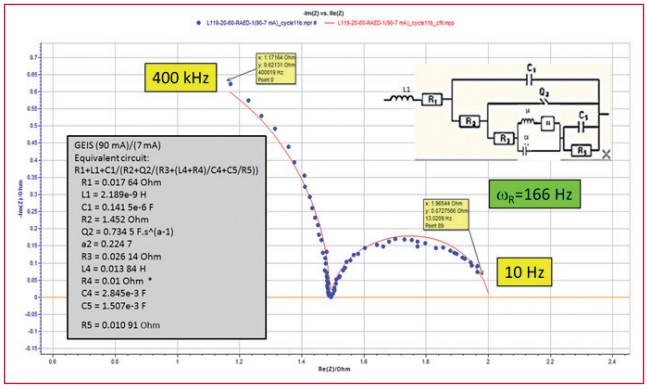

FIGURE 5C In situ Galvanostatic Electrochemical Impedance Spectroscopy on Sample L119(20-60). Excess-off before perturbing

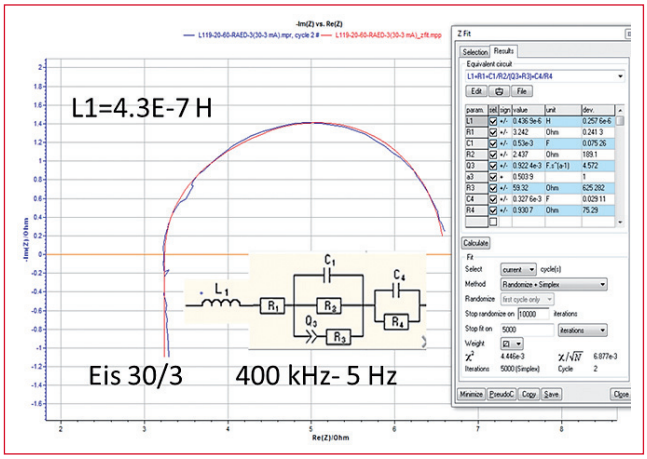

FIGURE 6 GEIS, 30mA/3mA 400 kHz-5Hz: Excess-Off

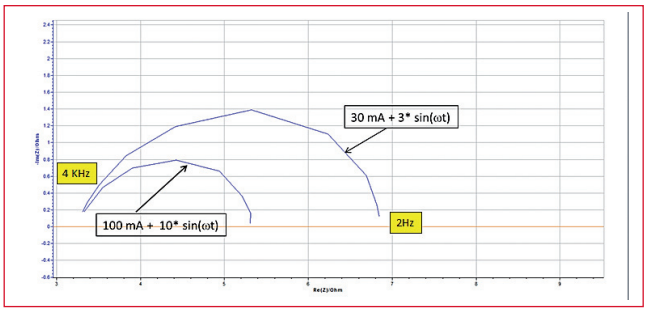

FIGURE 7 GEIS performed on inactive Pd electrode at two different current levels

similar samples revealed peaks in the PSD up to about 0.1 μm^{-1}. EDX (Energy-Dispersive X-ray) revealed that during the excess Fe, Cu and Pt were on the electrode surface.

Figure 9 shows a TEM image of the nanoporous nature of the "rice" structures created on sample L119(20-60).

Two additional samples from the same PdRh lot were investigated and were found to be totally inactive regarding the appearance of excess power. No evidence of specific surface contaminants and specific structures was observed on these two samples.

It is noteworthy to analyze the evolution of current and voltage, in galvanostatic mode, during the excess power production. A small oscillation of both current and potential was observed during the excess.

Figure 10 shows the sine wave behavior of current and

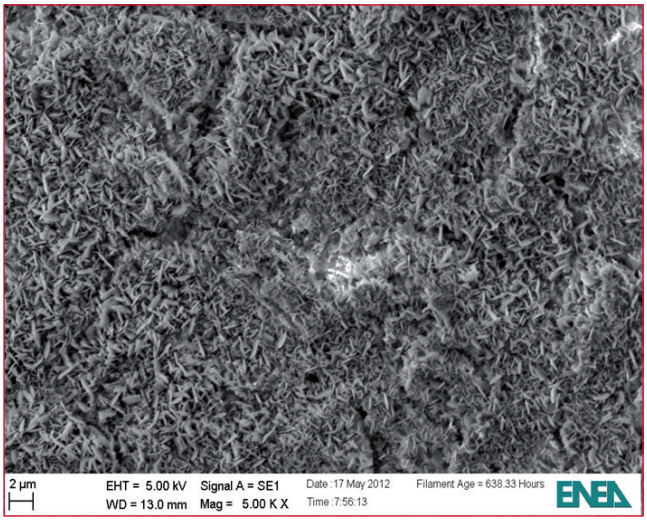

FIGURE 8A SEM image of the electrode surface of L119(20-60) as it was during production of excess power

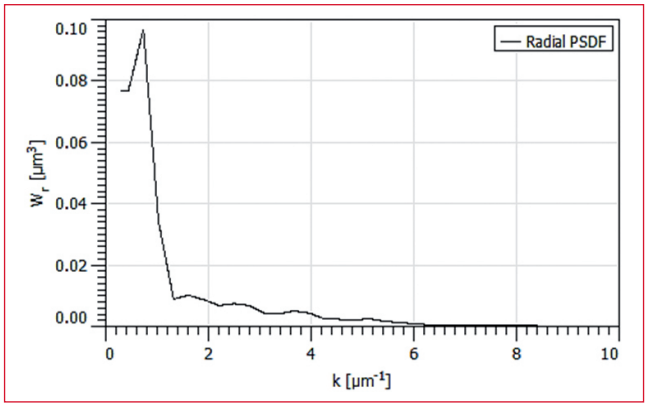

FIGURE 8B PSD of the surface shown in Figure 8a

overvoltage, reflecting clear electrochemical instability. Such a scenario is pointing towards morphology changing of the surface and pattern formation during the electrolysis [11].

We may also observe an additional signal at a higher frequency nested on the carrier wave. The carrier wave frequency is in the order of mHz. The existence of a not well resolved signal nested on the carrier wave is indicative of the existence of higher frequency mechanisms behind or beyond the observed behavior. For such a reason the high frequency region above 1 GHz needs to

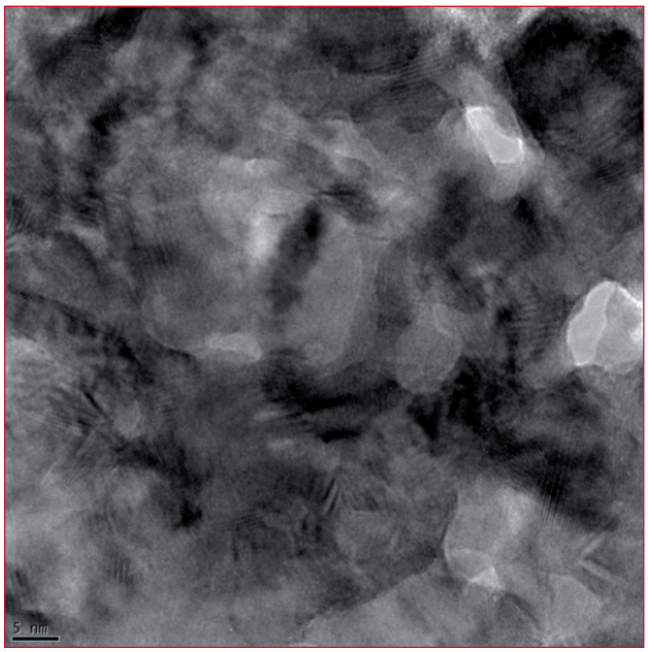

FIGURE 9 Nanoporous detail of "rice" structures observed on sample L119(20-60) as was during the excess power event (analysis performed by RE Research)

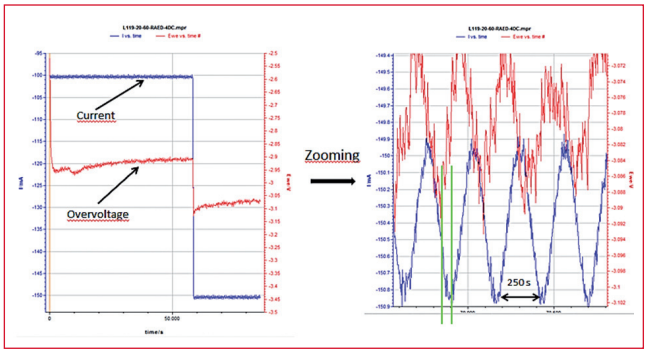

FIGURE 10 Current and overvoltage evolution during 40% excess power

be investigated.

Electrochemical literature [12] describes high characteristic frequency conditions for partially blocked porous electrodes, however there are several mechanisms, not necessarily purely electrochemical, that could produce high frequency signals at electrode interfaces. Nevertheless, although high frequency systems are assumed to exist in electrochemical systems, the literature explicitly mentions that proper instruments to study such specific electrochemical phenomena have not been conceived and realized yet. In the following we will present an original approach to such a very challenging frontier research.

Radio Frequency signal emission during excess power production close to 100 GHz

As described above, not only preliminary theoretical considerations but also some experimental evidences [8,13] suggested to seek for high frequency RF signals during excess power production into electrochemical cell. Very high frequency signals measurement, from tens of GHz up to a fraction of THz, into an electrochemical device, is not a simple matter. A proper measurement chain was conceived in ENEA in order to perform such a very challenging task by using a spectrum analyzer (20 Hz-3.6 GHz), manufactured by National Instruments. Besides providing its support to develop the relevant control software, this company also delivered the training on RF measurements.

In order to test the system, the RF spectrometer was connected to the reference electrode by means of a coaxial SMA type cable and the cell was powered by using a Biologic electrochemical spectrometer model SP240. A sine signal was applied from 20 kHz up to 2 MHz and was perfectly detected by the RF spectrometer connected to the reference electrode. Such a test confirmed the possibility to study the interface potential with this measurement chain without any significant disturbance from the electrochemical environment. One of the critical aspects in studying high frequencies is represented by the practical impossibility of having a high frequency signal, in the order of a fraction of THz, moving from the inside of an electrochemical apparatus to the measurement device, i.e. the spectrum analyzer. For such a reason a miniaturized frequency down converter (DWC) was designed and realized by Anonymous Industry (AI).

Such a small device (10mm x 10mm x 5mm ca.) can be introduced inside the electrochemical cell between one anode and the cathode. The DWC was conceived to have an internal clock at about 80 GHz. The device extracts the frequency difference between the input signal and

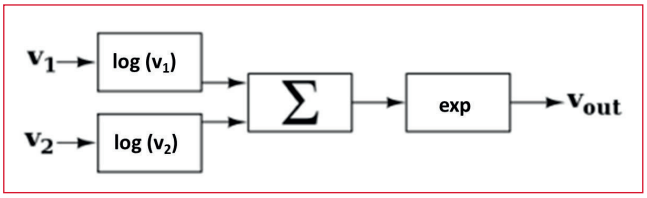

FIGURE 11 Schematic Block diagram of the Down converter: V1 is the RF signal, V2 is the internal signal at about 80 GHz; the exponential of the sum of the two signal logarithms gives a signal containing the frequency differences of the two inputs

its internal clock, and sends such a signal difference to the spectrum analyzer. Then, for instance, if there is an 83 GHz signal produced at the electrode the DWC sends the spectrometer an 83-80 = 3 GHz signal.

Obviously the spectrometer reads contemporaneously signals in the range 20 Hz-3.6 GHz and signals approximately in the range 80-83.6 GHz (76.4-80 GHz), however the two regions can be identified since if the DWC is not powered it may "read" only the signals in the basis band, i.e. 20 Hz-3.6 GHz. The difference between the two spectra (powered and non-powered) given by the DWC allows to identify the signal around 80 GHz.

Figure 11 shows the schematic block diagram of the down converter: V1 is the RF signal, V2 is the internal signal at about 80 GHz; the exponential of the sum of the two signal logarithms gives a signal containing the frequency differences of the two inputs.

Figure 12 shows the block diagram of the experimental set-up. The electrochemical cell is a closed cell with a catalyst inside of it that recombines the oxygen and deuterium produced by the electrolysis. The pressure inside the cell is monitored by a liquid column pressure gauge. The electrodic system is the typical ENEA design [3-5], composed by a palladium cathode between two platinum or platinated stainless steel anodes. The cell works within an isoperibolic calorimeter equipped with a DAC and a power supply (galvanostat), both designed and realized by (AI).

Two coils, producing both a short period magnetic pulse (in the order of a Tesla) and an acoustic shock wave (due to the magnetic pulse), are outside the cell. This device, too, was conceived and produced by (AI).

During the experimental campaigns described below,

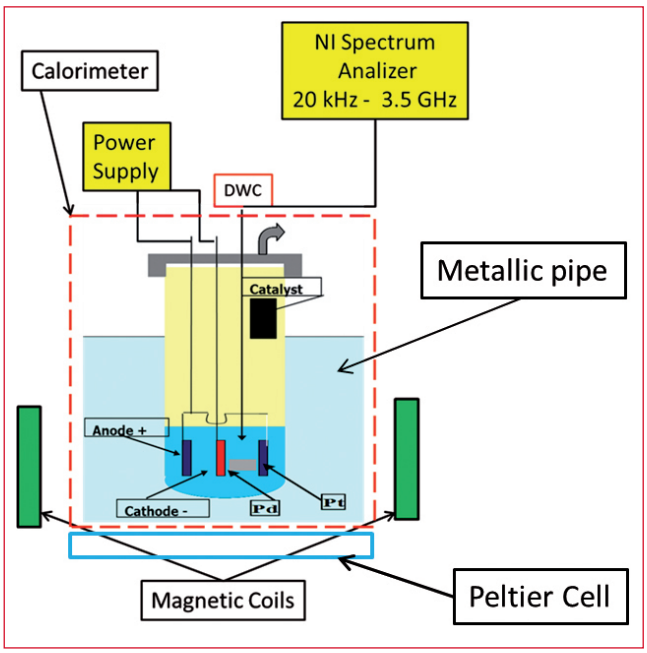

FIGURE 12 Block diagram of the experimental set-up

the thermal behavior of the system during the electrochemical loading and the magneto-acoustic triggering was simply followed by only measuring the cell temperature. The DWC is between one anode and the cathode and is connected with the spectrum analyzer by means of a SMA coaxial cable. Several palladium electrodes have been prepared in ENEA in order to perform the experiment. All the electrodes have been produced by using the ENEA process to guarantee a very high solubility of the hydrogen isotopes; some electrodes have been obtained by properly doping the palladium with platinum and other elements in order to enhance the probability to have the occurrence of the effect. All samples have undergone chemical etching in order to obtain the surface morphology considered as a necessary condition to observe the phenomenon [3-5].

First experimental campaign

The first experiment was performed by using sample L122(120-160), which underwent electrochemical loading for about 12 hr at 20 mA. Then the cell was moved

into the calorimeter equipped with the pulsed magnetic field and the current was increased at 24 mA. Seven cycles of pulsed magnetic field (40 pulses each) were applied; the time elapsed during a magnetic stimulus cycle was about 3 minutes. Yet, during this experimental campaign and also during the second (see next section) the calorimeter was not operated and the thermal behavior of the system was monitored just reading the electrolyte temperature on the wall of the cell.

The spectrum resulting from data acquisition at the beginning of the experiment was perfectly reproducing the background (see Figure 13), and the temperature on the external side of the cell wall was almost constant at about 31 °C. During cycle No. 7 of the magnetic stimulus, a clear RF signal was revealed by the spectrometer and the electrolyte temperature started to rise of several °C in about 20 min.; the spectrum is shown in Figure 14 and contains the signal into the basis band up to 1 GHz and the signal around 79-81 GHz. We may observe that the signal level reached values around -40 dBm well above the background. The electrolyte temperature increase is ascribed to an anomalous excess power production significantly larger than the input power.

During the effect an external multimeter also measured the voltage of the cell and the value was the same given by the data acquisition system. The magnetic field trigger device was switched off and disconnected, and so was the peltier cell of the calorimeter; nonetheless the excess survived until the power supply of the electrochemical cell was switched off and the cell was disconnected. In conclusion a thermal anomaly, along with a clear increase in the electrochemical cell temperature, typical of an excess power production, was observed in coincidence with the RF signal emission. Figures 15 and 16 are the screen copy of the RF spectrometer before and during the excess power, obtained by sample L122(120-160). The same electrode was operated again on the following day, before restarting the cell was cleaned and the electrolyte was replaced with a new one. The loading was carried out at 53 mA. With such a current level 6 cycles of magnetic pulses were applied, then the current was reduced to 24 mA and during the second cycle of magnetic pulses, at this current level, both excess power and RF signal were observed again. The RF spectrum is shown in Figure 17, the electrolyte

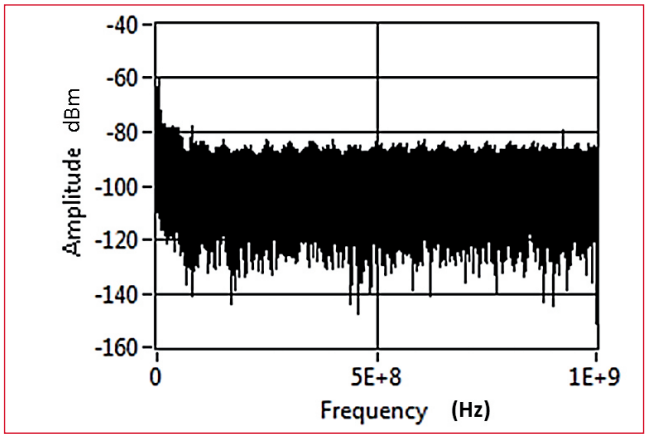

FIGURE 13 Background spectrum up to 1 GHz of sample L122(120-160) before cycle No.7 (10 points average)

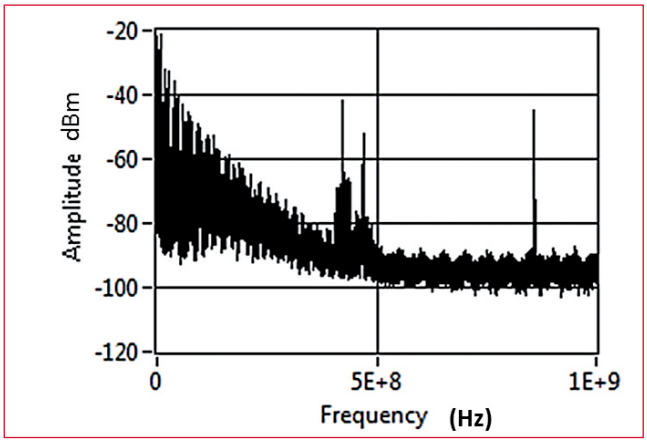

FIGURE 14 RF Spectrum up to 1 GHz of sample L122(120-160) during heat excess (10 points average)

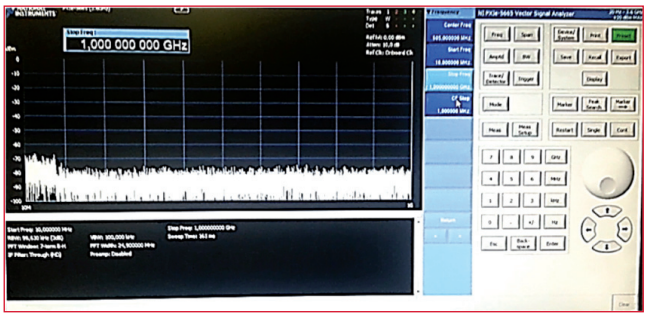

FIGURE 15 Image of the RF spectrometer screen before the excess power event (sample L122(120-160))

FIGURE 16 Image of the RF spectrometer screen during the excess power. Sample L122(120-160)

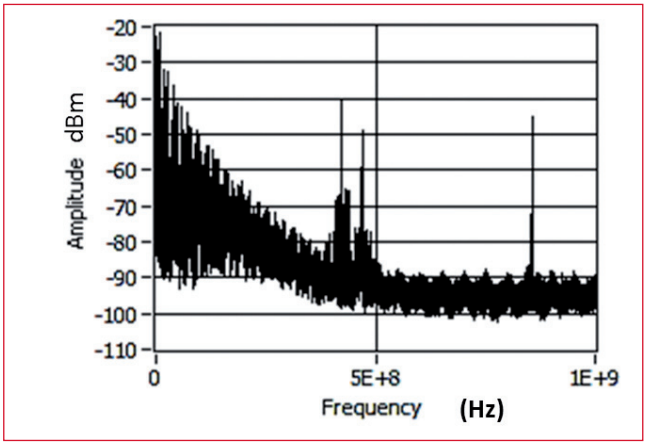

FIGURE 17 RF spectrum up to 1 GHz observed during the second run of sample L122(120-160) (10 points average)

temperature increase was the same as the one observed in the previous run.

Second experimental campaign

A second experimental campaign was carried out three weeks later. Another electrode L122(308-366), belonging to the L122 lot, was tested. The current was fixed at 53 mA and during the magnetic pulses cycle No. 4 RF emission was observed but without any evidence of cell temperature increase. Figure 18 shows the spectrum observed with the down converter powered: we observe at least 6 peaks including the basis band. To extract the signal into the basis band the powering of the down

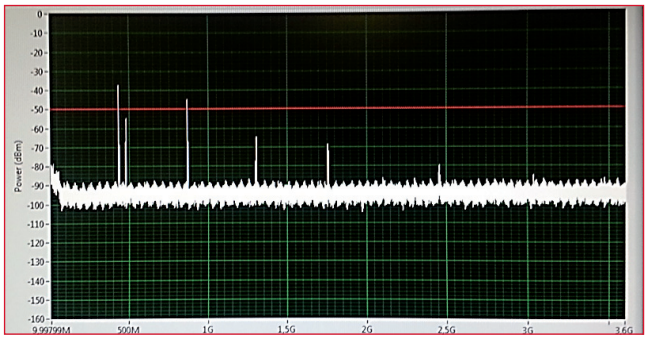

FIGURE 18 L122(308-366) spectrum observed with the down converter powered including both signals 10 MHz-3.6 GHz and 76.4-83.6 GHz

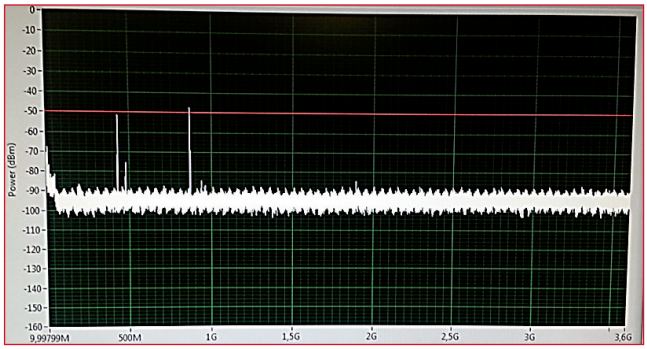

FIGURE 19 L122(308-366) spectrum observed with the down converter not powered, it includes the basis band signal only

converter was switched off and the spectrum modifies as shown in Figure 19. The spectrum in the range 76.4-83.6 GHz may be obtained by means of the difference of the two spectra.

Also sample L122(160-200), which gave a clear temperature increase and RF signal emission during the first experimental campaign was experienced again. Platinum anodes have been used for a new run and the current was fixed at 53 mA. After 8 cycles of magnetic pulses at 53 mA and 8 at 24 mA neither excess power nor RF signals were observed. Then the current was increased up to 107 mA and maintained at such value for a whole night in order to improve (presumably) the loading.

On the following day, 5 cycles were performed at 97 mA without any effect, then the current was reduced to 53 mA and after 5 cycles at this current level both

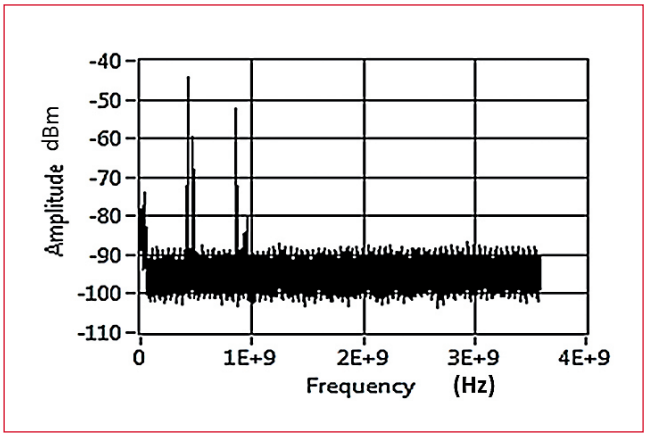

FIGURE 20 RF spectrum given by sample L122(160-200) during excess with non-powered down converter (basis band)

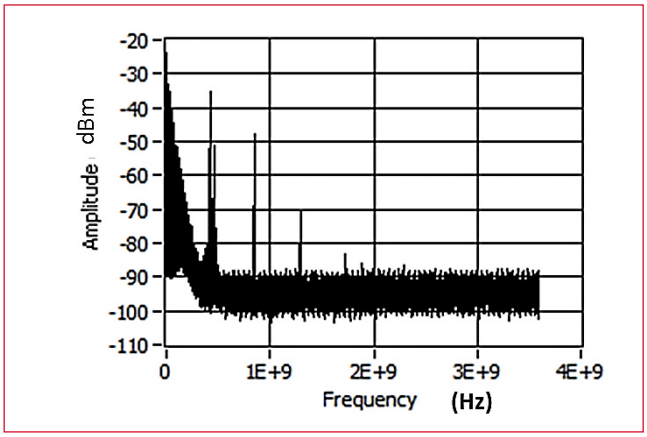

FIGURE 21 RF spectrum given by sample L122(160-200) during excess with powered down converter (including basis band and 76.4-83.6 GHz range)

Electrode	Lot	Electrolyte (0,1M Li)	Current mA	Notes	RF	Excess
Steel	NA	H_2O	53	NA	No	No
Steel	NA	D_2O	53	NA	No	No
L124(10-50)	Pd90/Rh10 (Al)	H_2O			No	No
L127(20-130)	H.M. + Pt	H_2O			No	No
L128(105-145)	H.M. + Pt	D_2O			No	No
L128(145-185)	H.M. + Pt	H_2O			No	No
L58(165-200)	J. M. MM29560	H_2O			No	No
L93(110-150)	A. A. 307622	H_2O			No	No
L95(50-90)	A. A. 307622	D_2O			No	No
L121(90-130)	Pd90/Rh10	D_2O			No	No
L125(170-206)	H.M. 2108539 + Pt	D_2O			No	No
L122(120-160)	Pd+Pt*	D_2O	24		Yes	Yes
L122(120-160)	Pd+Pt*	D_2O new	53		Yes	Yes
L122(160-200)	Pd+Pt*	D_2O	53		Yes	Yes
L122(160-200)	Pd+Pt*	D_2O	53	Charged at 107 mA	Yes	Yes
L122(236-272)	Pd+Pt*	D_2O	53		No	No
L122(308-366)	Pd+Pt*	D_2O	53		Yes	No
L137(100-140)	Pd+Pt*	D_2O	53		No	No
137(180-216)	Pd+Pt*	D_2O	107	Anode Pt	No	No
L137(60-100)	Pd+Pt*	D_2O	107	Anode Pt	Yes	No
L137(60-100)	Pd+Pt*	D_2O	107	Anode Pt	Yes	Yes

TABLE 1 Synoptic summary of the experimental results. If not specified in the table the anode was platinated stainless steel

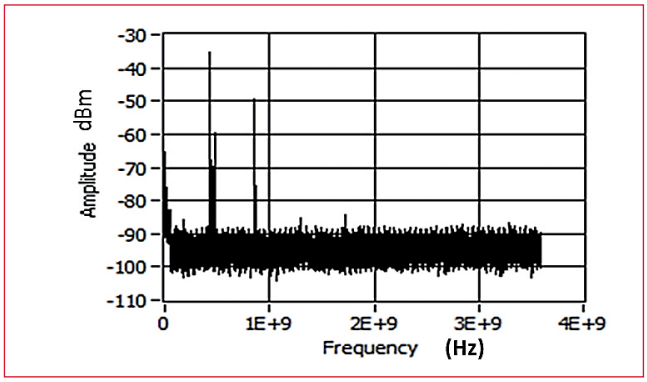

FIGURE 22 RF spectrum produced by sample L137(60-100) without any production of excess heat

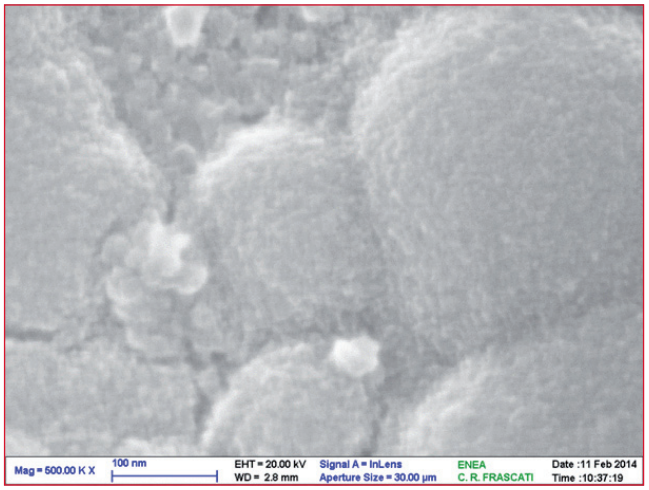

FIGURE 23B L122 (120-160) surface at FE Mag 500k

electrolyte temperature increase and RF emission were observed. Also in this experiment, during the event, the down converter powering system was switched off in order to identify the basis band signal.

Figure 20 shows the RF spectrum given by sample L122(160-200) during excess by keeping the down converter non-powered (basis band). Instead, Figure 21 shows the RF spectrum given by sample L122(160-200) during excess and powering the down converter (including basis band and 76.4-83.6 GHz range). It must be highlighted that some handling of the experimental set-up, i.e. opening and closing the insulating bell, de-

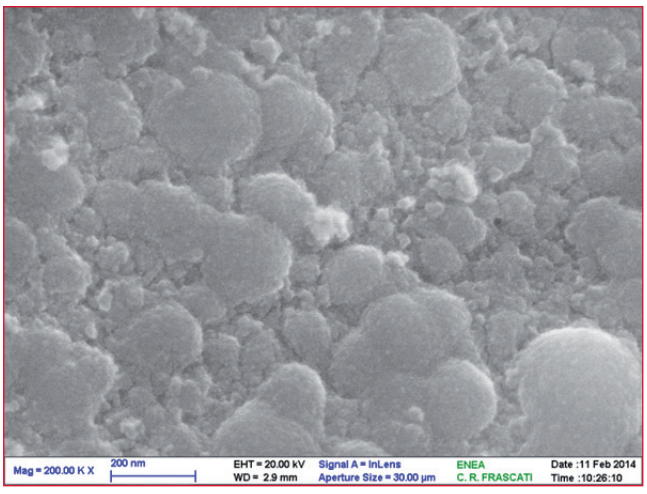

FIGURE 23A L122 (120-160) surface at FE Mag 200k

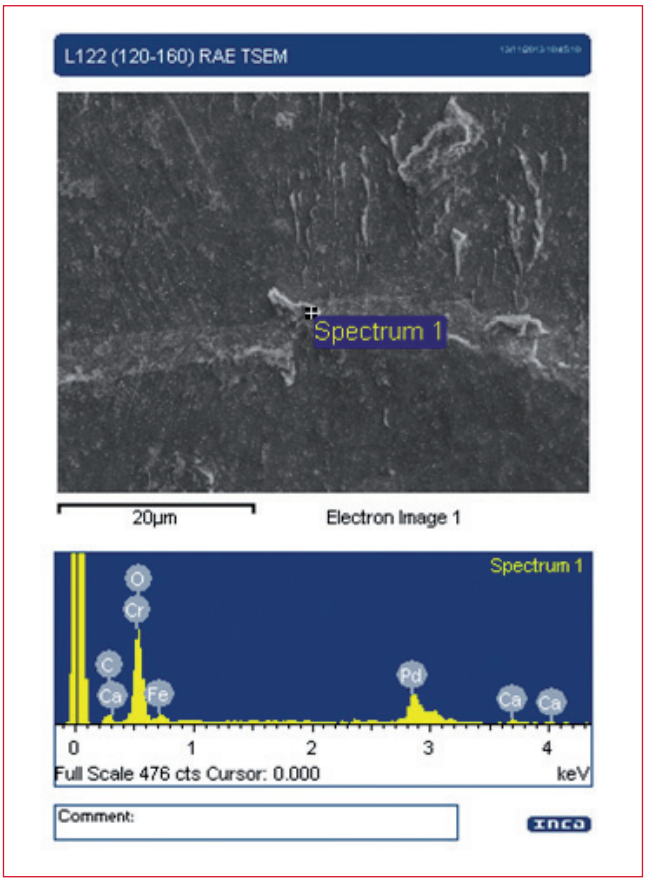

FIGURE 24A EDX point 1 L122(120-160)

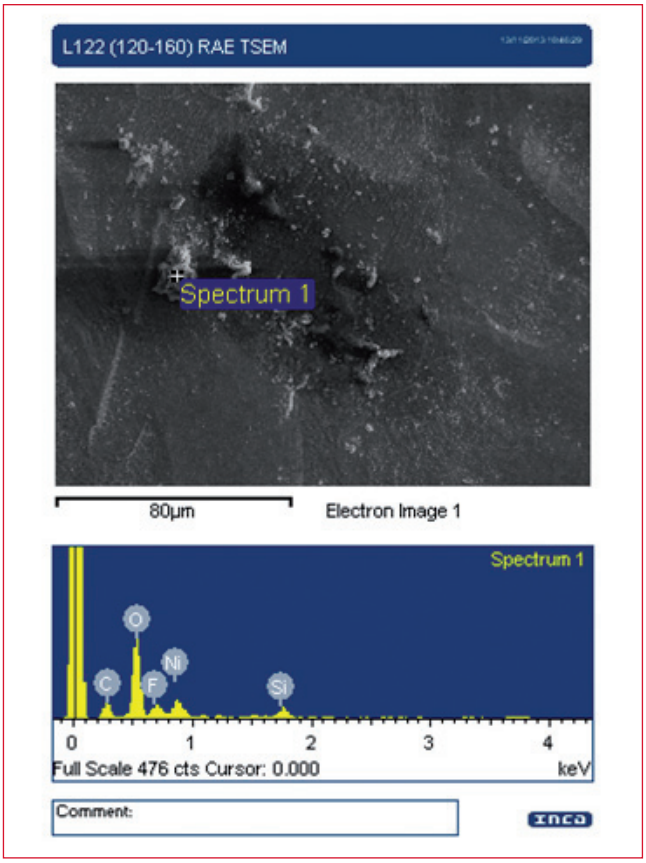

FIGURE 24B EDX point 2 L122(120-160)

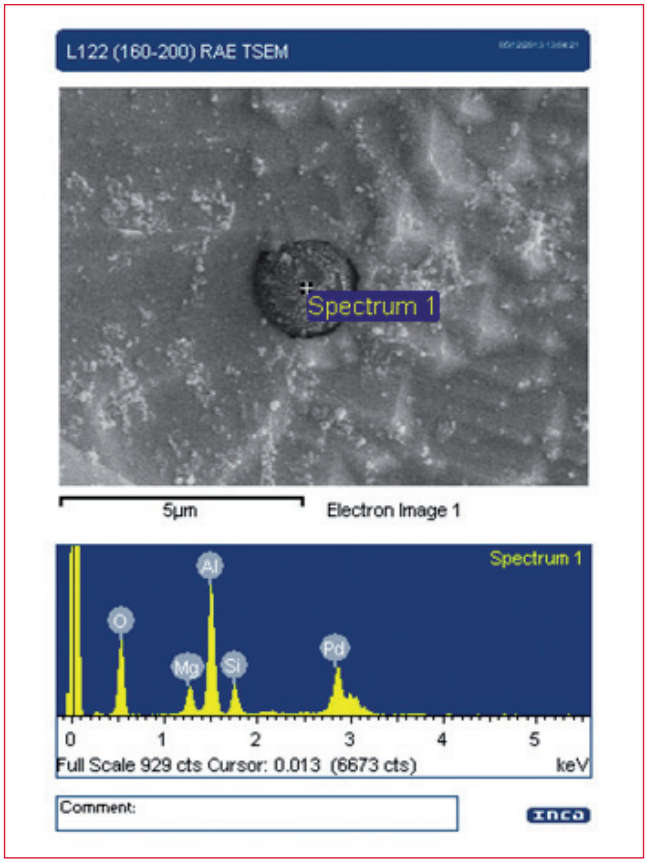

FIGURE 26 L122(160-200) EDX

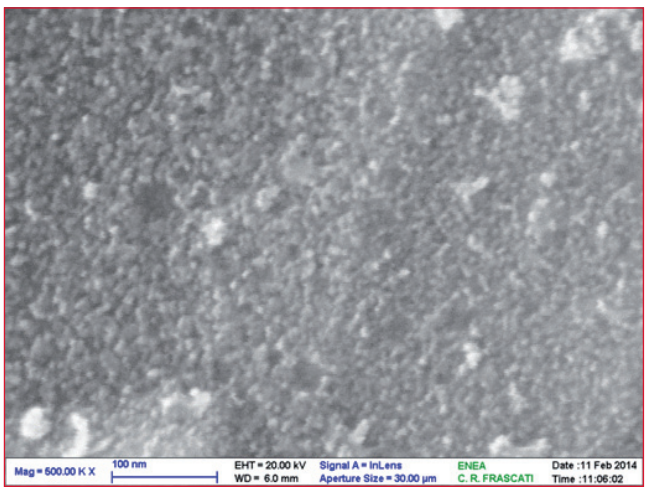

FIGURE 25 FE L122(160-200) Mag 500k

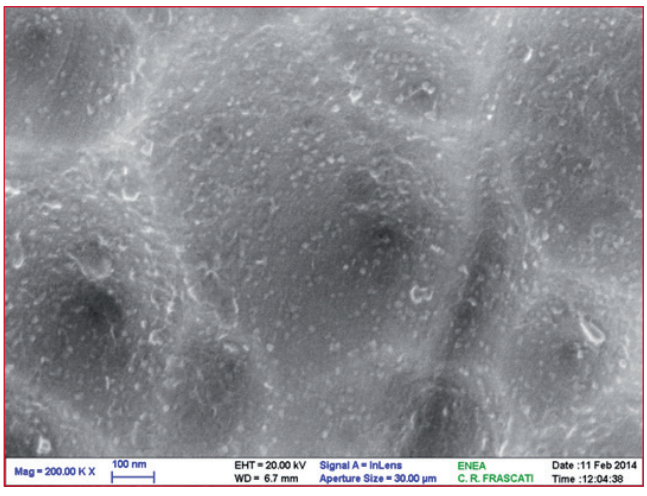

FIGURE 27 L122(308-366) 200k Mag

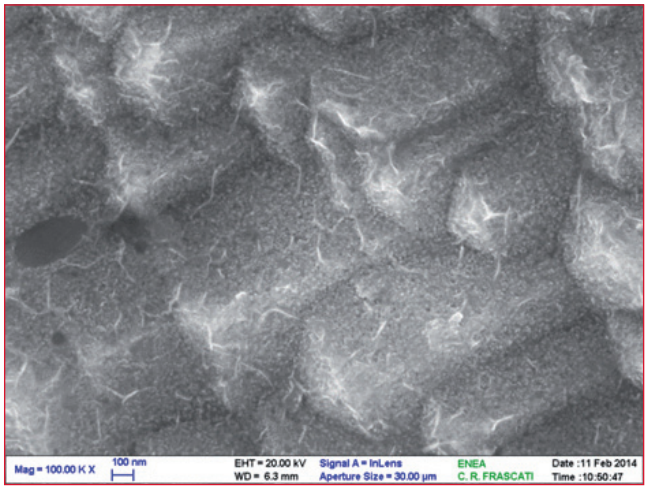

FIGURE 28A L137(60-100) 100k Mag (site 1)

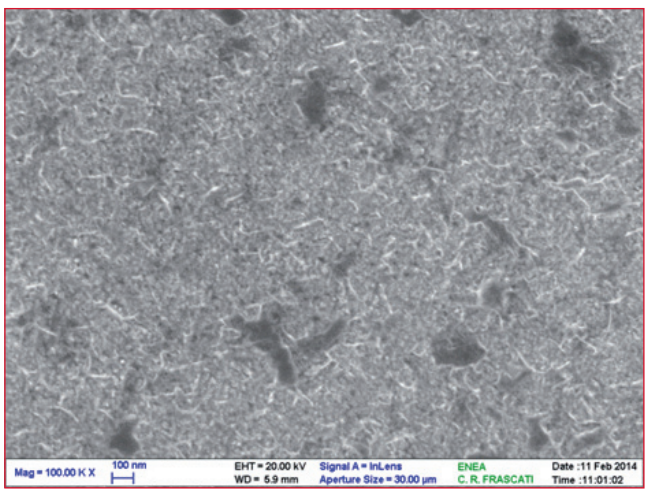

FIGURE 28B L137(60-100) 100k Mag (site 2)

stroyed both the heat excess and the RF signal, but a further cycle of pulses was able to reproduce both effects. The last active electrode tested was L137(60-100), also operated with platinum anodes. The behavior was similar to that of sample L122(308-366). The applied current was 107 mA and during magnetic pulses cycles a RF signal was observed without any thermal anomaly. It is noteworthy that only L122 and L137 lots have been able to give excess power and RF emission, both lots being prepared by Pt and other doping elements exactly in the same amount. Also further loading sample L137(60-100) resulted in anomalous heat production and RF emission. Figure 22 shows the spectrum during RF emission from sample L137(60-100) without any temperature increase. From the previous data it is clear that RF emission is not a consequence of the excess heat production but, perhaps, the cause. Then, by comparing the spectra shown in Figures 18 and 19 we have been able to identify the basis band peaks and the peaks within ~77-83 GHz range that cannot be ascribed to the occurrence of the effect, due to the absence of anomalous power production. Sample L137(60-100) was left loading at about 100mA for a whole night and triggered again by magnetic pulses. Under such a stimulus it produced a very robust excess power of the same amplitude of samples L122(120-160) and L122(160-200). Table 1 shows a synoptic summary of the electrodes used for such a study.

Status of the electrodes

After the experiments some samples (active and non-active) have undergone microscope analysis. In particular SEM, EDX and Field Emission have been used to characterize the status of the surface.

Figures 23a and 23b show the surface of sample L122 (120-160) after the experiment for two different magnification values (200 and 500, respectively). We may observe coverage of small spheres having a size ranging from 200 nm down to less than 100 nm. In Fig 23b we may observe a porous structure at small scale. A similar structure was observed at small scale also on sample L119(20-60) (see Figure 9).

EDX analysis (Figures 24a and 24b) reveals a significant amount of Si, Cr, Al and Fe (same as L119(20-60)).

The surface status of sample L122(160-200) is shown in Figure 25. Spheres having a size less than 100 nm can be identified as well as coverage of nano-deposit.

EDX analysis of sample L122(160-200) is shown in Figure 26 and reveals a spectrum of contaminants.

Figure 27 shows that also sample L122(308-366) has a clear nano-deposit on the surface nested on larger-sized structures that are always in the order of some hundreds of nm.

Sample L137(60-100) (see Figures 28a and 28b) has surface features very close to the ones observed on sample

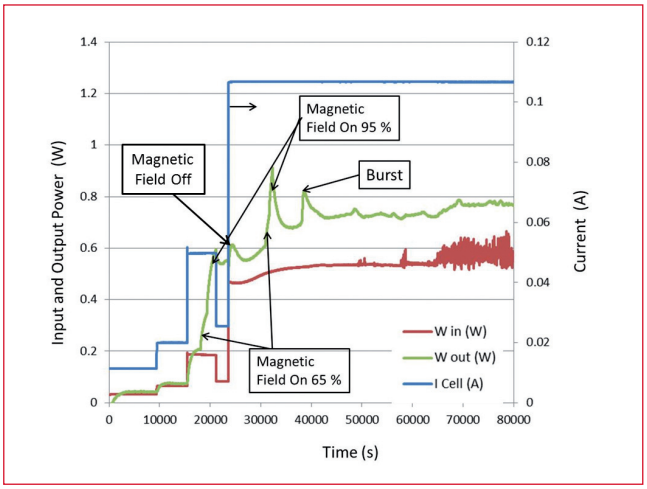

FIGURE 29 Evolution of the input and output power during the experiment performed by using sample L137 (300-340) was belonging to the same active lots used during the first and the second experimental campaigns

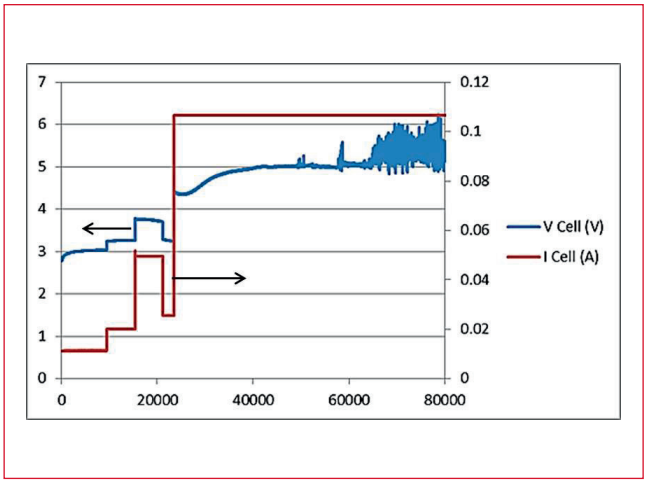

FIGURE 30 Cell voltage (blue) and cell current (red) during experiment L137 (300-340)

L122(160-200), consisting of nano-deposits.

Replication with ENEA hardware and calorimetric measurements

The experiment with a pulsed magnetic trigger, described above, was replicated by using a proper magnetic hardware developed in ENEA. During the experiment a calorimetric measurement was carried out, too.

Two coils have been designed to give short period magnetic pulses in the order of one Tesla. The input power is calculated as the scalar product between the current and the voltage (closed cell). The output power is estimated by reading the voltage signal across a Peltier cell placed between the bottom of a metallic pipe containing the cell and a heat sink. Since the Peltier voltage signal is proportional to the thermal load into the cell, a calibration allows to translate the voltage in terms of output power. A Lab View Program was developed both to control the power supply (the electronic board) and to perform the data acquisition by reading the data directly from the board. The software was also able to perform a calibration correction during the run. The Peltier isoperibolic calorimetric apparatus, described above, was calibrated with light water electrolyte (LiOH) with and without applying the magnetic field, in order to estimate the effect on the calorimeter produced by the heating of the coils (160 mW and 450 mW at 65% and 95% of the maximum intensity of the magnetic field, respectively). The palladium cathode was sample L137 (300-340), belonging to the same active lots used during the first and the second experimental campaigns. Such a sample was etched exactly as the active samples previously used. We may follow the evolution of the experiment with the help of Figure 29. Initially, the current was first fixed at 16 mA and then at 24 mA, and no excess power was observed. Then the current in the cell was increased up to about 50 mA and the magnetic field was applied at 65% of the maximum intensity (close to 1 Tesla), at about 18000 sec elapsed time. After some hundreds of pulses the magnetic field was increased up to 95% of the maximum intensity, approximately at 20000 sec elapsed time. The expected increase in the output power due to the coils heating is the same observed and quoted during the calibration. During the 95% magnetic pulse the current was reduced down to 24 mA for a short time, then the magnetic trigger was switched off and the current increased up to 107 mA (the same loading current giving excess with sample L137(60-100)), approximately 24000 sec elapsed time. We may observe a decrease in the output power, due to the switching off of the magnetic trigger at around 25000 sec elapsed time, and then an increase in both in-

put and output power due to a spontaneous increase in the cell voltage (see Figure 30). In any case it should be observed that, after applying the magnetic field the first time, an increase in the cell voltage occurred and a small excess power came up (100 mW) . The pulsed magnetic field was applied again first at 65% and then at 95%. After applying the magnetic field the second time, the excess event increased up to about 200 mW and a burst occurred, giving an excess power up to about 50%. We may observe that after the burst, the excess power survives, the cell voltage becomes very noisy and also the current shows a ripple (out of the scale of Figure 30). This effect is often observed during excess power production. A similar experiment was carried out on a sample belonging to the same lot but prepared with a different chemical etching, and no excess of power was observed.

Conclusions

The experimental data show that excess power is characterized by a dramatic changing of the electrochemical interface, leading to a resonant phenomenon occurring into identified resonating structures, which highlights the importance of investigating surface/interface equivalent electric circuits. In addition it turns out that nanoporous structures have been identified on the active samples. An RF signal emission has been observed during the excess power production but such a signal has been obtained also when the excess power was absent, showing that RF emission is not the effect of the excess but perhaps the cause. Very often electrochemical instability is observed in coincidence with the onset of the effect. Even if the role of the high frequency source (DWC) is still under study, the magnetic (acoustic) trigger – that seems to act on the identified resonating structure – is very effective for obtaining the onset of the effect since during the three experimental campaigns, including the replication with ENEA hardware, it has given a significant reproducibility when active lots (i.e. properly doped Pd samples) have been used. This was obtained by doping a rough palladium originally inactive. Such a result that in any case should be considered as a first step is pointing in the direction of the complete control of the effect and its definition.

Notes

The hardware provided by A.I. was tested by the manufacturer and operated as it was.

Acknowledgements

The authors wish to acknowledge the very important support received by Dr. Stefano Concezzi, Dr. Augusto Mandelli, Dr. Daniele Persia and Dr. Marco Castellano from National Instruments, and also by Dr. P.J. King and Dr. Mason Guffey from RE Research.

references

[1] M. McKubre et al., "Excess Power Observations in Electrochemical Studies of the D/Pd System; Influence of Loading", Proc. Third Intern. Conference on Cold Fusion (ICCF3), Nagoya, Japan, October 21-25, 1992, pp. 5-19.

[2] G.K. Hubler, "Anomalous Effects in Hydrogen-Charged Pd – A Review", Surf. Coatings Tech., 201 (2007) 8568.

[3] V. Violante et al., Material Science on Pd-D System to Study the Occurrence of Excess of Power, Proc. ICCF-14, Washington DC 10-15/8/2008, Vol 2, pp. (429-436).

[4] V. Violante et al., Evolution and progress in material science for studying the Fleischmann and Pons effect (FPE), Proc. ICCF-15 Oct 5-9 2009, Rome, Italy, pp. 1.

[5] V. Violante et al. The study of the Fleischmann and Pons effect through the materials science development. Proceedings of the XVI International Conference on Condensed Matter Nuclear Science. Chennai, India, Feb 6-11 2011, pp. 313.

[6] D.L. Knies, V. Violante, K.S. Grabowski, J.Z. Hu, D.D. Dominquez, J.H. He S.B. Qadri and G.K. Hubler, "In situ Energy-Dispersive X-ray diffraction study of thin Pd foil at D/Pd and H/Pd ~1", Proc. ICCF15, Rome, Italy, Oct., 2009.

[7] D. L. Knies, V. Violante, K. S. Grabowski, J. Z. Hu, D. D. Dominguez et Al., In-situ synchrotron energy-dispersive x-ray diffraction study of thin Pd foils with Pd:D and Pd:H concentrations up to 1:1, J. Appl. Phys., 112, 083510 (2012); doi: 10.1063/1.4759166.

[8] V. Violante, E. Castagna, S. Lecci, F. Sarto, M. Sansovini, T. D. Makris, A. Torre, D. Knies, D. Kidwell, K. Grabowski, D. Dominguez, G. Hubler, R. Duncan, A. El Boher, O. Aziz, M. McKubre, A. La Gatta, Excess of Power During Electrochemical Loading: Materials, Electrochemical Conditions and Techniques, Proceedings ICCF18 Int. Conference on Condensed Matter Nuclear Science, 20-25 Jul 2013, Columbia (MU) USA. In press.

[9] D.D. Dominguez et al., Are Oxides Interfaces Necessary in Fleischmann and Pons Type Experiments?, Proceedings of the XVI International Conference on Condensed Matter Nuclear Science. Chennai, India, Feb 6-11 2011, pp. 53.

[10] D. Knies et al, Differential Thermal Analysis Calorimeter at the Naval Research Laboratory, Proc. ICCF- 15 Oct 5-9 2009 Rome, Italy, pp. 11.

[11] Kazuhiro Fukami et Al. , General Mechanism for the Synchronization of Electrochemical Oscillations and Self-Organized Dendrite Electrodeposition of Metals with Ordered 2D and 3D Microstructures, J. Phys. Chem. C, 2007, 111, 1150-1160.

[12]M.E. Orazem, B. Tribollet, Electrochemical Impedance Spectroscopy, John Wiley and Sons, 2008, Hoboken (NJ), pp. 157.

[13] D. Dominguez, D.A. Kidwell, G.K. Hubler, S.F Cheng, M.A. Imam, K.S. Grabowski, D.L. Knies, L. De Chiaro, A.E. Moser, J.H. He, V. Violante, 17° Conference on Condensed Matter Nuclear Science, Daejeon, (Korea) 12-17 August 2012. http://lenr-canr.org/acrobat/DominguezDanomalousr.pdf